Design and Performance Analysis of Single-phase Axial Flux Permanent Magnet Motor for Coaxial Cascade

Chu Wang, Xiaowei Hu, Xiaoya Wang, Weiwei Geng, Qiang Li and Jingning Hou
Nanjing University of Science and Technology
Nanjing 210094, Jiangsu Province, China
Tel.: +86 – 15850724704
Fax: +(025)84315468-7085
E-Mail: gww@njust.edu.cn
URL: http://www.njust.edu.cn/

Keywords

« Axial machines », « All Electric Aircraft », « Electrical machine », « Finite-element analysis », « Permanent magnet motor », « Synchronous motor ».

Abstract

This paper is about the modeling, design and verification of single-phase axial-flux permanent magnet (AFPM) motor for coaxial cascade. The topology principle with yokeless and segmented armature (YASA) is proposed and discussed. The single-phase AFPM motor is designed and coaxially cascaded for forming a multiphase AFPM motor to compare with three-phase AFPM motor. The comparative results show that the three-phase AFPM motors formed with coaxial has higher power density and fault-tolerant ability.

Introduction

In recent years, with the rapid development of electric aircraft, the electric propulsion system of many electric aircraft needs higher power density, torque density and efficiency due to the limitation of installation space and weight [1]-[3]. High power / torque density motor has always been the key basic component of electric propulsion system. Because of its compact axial construction and high torque density, AFPM motors are widely concerned in electric vehicles, aerospace and other fields [4]-[6].

However, there are still significant challenges in the application of three-phase AFPM motor in the case of rotorcraft or UAV. For the traditional three-phase AFPM motor, it is difficult to meet the general space requirements of rotor wing integration due to the high length-diameter. Furthermore, the electro-magnetic coupling among three-phase windings and winding short circuit. The polyphase AFPM motor system composed of single-phase multistage coaxial motor is suitable for applications with long axial length and can improve the fault-tolerance [7]-[12].

This paper presents a new topology of three-phase AFPM motor formed by single-phase AFPM motor coaxial cascade. Finite element method is used to compare the electromagnetic performance, torque capacity and fault-tolerance features between single-phase AFPM coaxial motor and traditional three-phase coaxial motor.

Description of AFPM motor with multiple single-phase coaxial cascade

The single-phase motor usually refers to the asynchronous AC motor. The single-phase AFPM motor proposed in this paper is used to connect three independent single-phase motors in series on the same shaft.

Fig. 1 shows the topology structure and equivalent magnetic circuit of single-phase AFPM motor. The solid line with arrow is the closed loop of the magnetic flux path generated by a pair of N and S poles. The specific magnetic flux path is described as follows. The magnetic flux starts from the N-pole

permanent magnet, passes through the air-gap, stator core and air-gap to the N-pole permanent magnet of another rotor mountain, then passes through the rotor core to form a closed magnetic circuit.

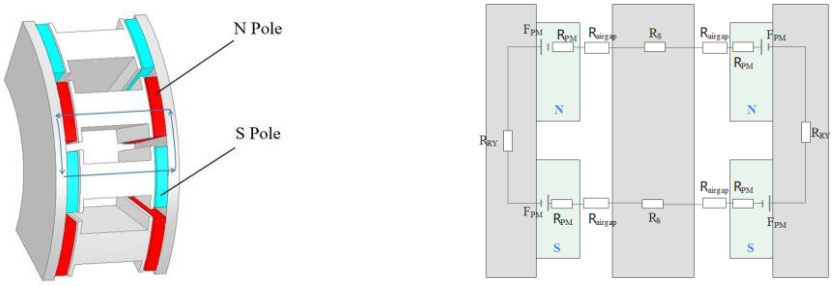

(a) Topological structure (b) Principle of magnetic flux path

Fig. 1: Topology principle of single-phase AFPM motor

Three coaxially cascaded motors are independently working at the same time to form an equivalent three-phase rotating magnetic field which is staggered in coaxial direction, as shown in Fig. 2. Consequently, there is no electromagnetic coupling and mutual inductance among phase windings. The required torque is generated with coaxial superposition of three independent single-phase motors. The explosive view and structure of three-phase motor for coaxial cascade are shown in Fig. 3.

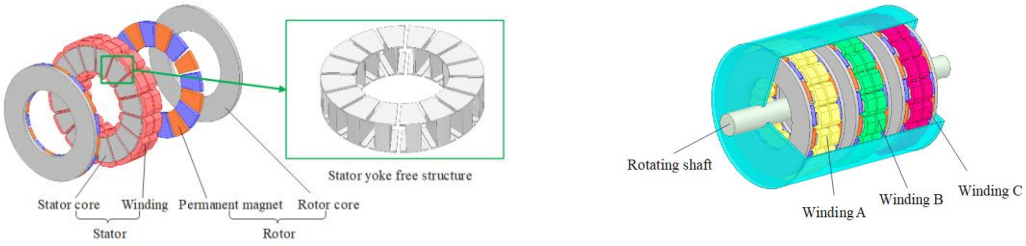

(a) Explosive view of single-phase AFPM motor (b) Structure of single-phase coaxial motor

Fig. 2: Schematic diagram of the single-phase motor for coaxial cascade

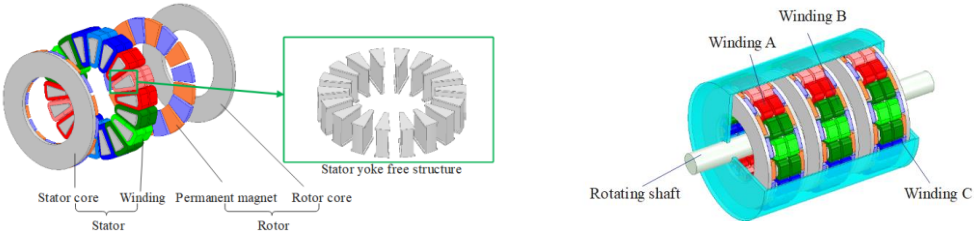

(a) Explosive view of three-phase AFPM motor (b) Structure of three-phase coaxial motor

Fig. 3: Schematic diagram of the three-phase motor for coaxial cascade

Design and modeling of AFPM motors

Each rotor axis of the rotor UAV is driven by an electric motor. The properly designed motor can achieve high mobility, has the advantages of small size and light quality, and can meet the basic requirements of UAV drive quickly and accurately. Table. I. shows the design requirements for a driving power matching for some kind of rotor aircraft. To better analyze the basic properties and advantages of single-phase AFPM motors, a 16-slot 16-pole AFPM motor was designed and cascaded to form a three-phase AFPM motor, compared to the conventional 16-slot 18-pole three-phase AFPM motor. ANSYS Maxwell software is used for finite element analysis and simulation model is established. In order to target theoretical calculation and simulation analysis, variables must be controlled so that the two AFPM motors have the same size, current density, slot filling factor, etc. Size parameters and winding information of the designed motor are shown in Table. II. It can be seen that compared with the

traditional three-phase AFPM motor, we have the same poles and different grooves, the materials of two motors and other structural parameters are both the same.

Table I: Motor design requirements

Parameter	Value
Continuous Output (kW)	5
Peak Power (kW)	10
Continuous Output Torque (N·M)	25
Peak Output Torque (N·M)	50
Rated Speed (rpm)	2000
Peak Speed (rpm)	3000
Effective Material Weight (kg)	＜3
The Efficiency	＞90%
Working Voltage (V)	36

Table II: The motor structure parameters

Parameter	Three-phase AFPM Motor	Single-phase Coaxial Motor
Slot Number	18	16
Pole Number	16	16
Outer Diameter of Motor (mm)	90	90
Inner Diameter of Motor (mm)	52	52
Air-Gap Length (mm)	0.5	0.5
Axial Length (mm)	33×3	33×3
Thickness of Permanent Magnet (mm)	3	3
Number of Turns	16	16
Number of Parallel Branches	1	1
Slot Filling Factor	0.6	0.6
Core Material	1J22	1J22
Permanent Magnet Materials	N52	N52

All core parts of single-phase coaxial motor and three-phase coaxial motor are made of the same material. In particular, it is pointed out that the stator core and rotor core are made of 1J22 material, and the permanent magnet is N52 rare earth permanent magnet with residual magnetism of 1.45 T. 1J22 is a high saturation magnetic induction strength iron diamond vanadium soft magnetic alloy. Due to the high saturation magnetic induction strength, the volume can be greatly reduced when making motors with the same power. Fig. 4 shows the magnetization curve of 1J22 material.

Comparative analysis of electromagnetic performance

a. Performance comparison at no load

Fig. 5 shows the waveforms of no-load back EMF of two motors, with RMS voltage of 18.65 V and 18.69 V respectively. It can be seen that the waveform of single-phase coaxial motor is more sinusoidal. Fig. 6 shows the phase back EMF at no load of the two motors. Among them, the phase voltage RMS values of single-phase motors and three-phase motors are 10.9V and 10.2V respectively. The waveforms of the two motors at load Fourier decomposition are shown in Fig. 7 .

Fig. 8 shows the air-gap flux density waveforms of single-phase AFPM motor and three-phase AFPM motor. It can be seen that the magnetic dense waveform of the single-phase motor is smoother. This is because the number of pole slots for a single-phase generator corresponds to each tooth. However, the

tooth groove of the three-phase motor makes the pole cannot correspond one to one, resulting in the magnetic leakage of the pole and the local magnetic density protrusion.

Fig. 9 shows the Fourier decomposition of air gap-flux density waveform. It can be seen that the fundamental amplitude BS of the air-gap magnetic density of single-phase coaxial motor and three-phase coaxial motor are both 1.2 T. The amplitude of the third and fifth harmonics of the three-phase AFPM motor are significantly higher than that of the single-phase coaxial motor.

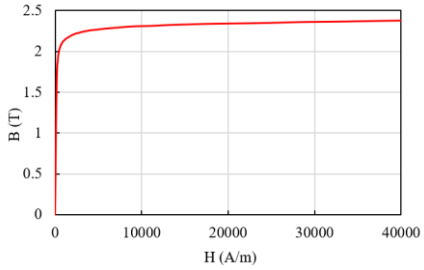

Fig. 4: 1J22 material magnetization curve.

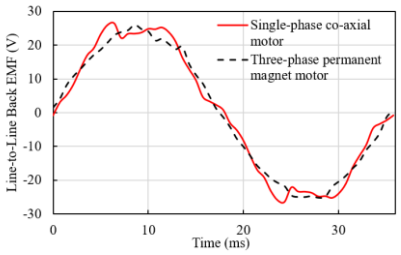

Fig. 5: Line-line back EMF at no load

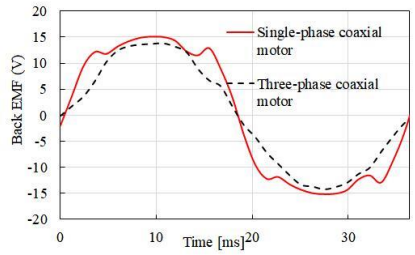

Fig. 6: Phase back EMF at no load

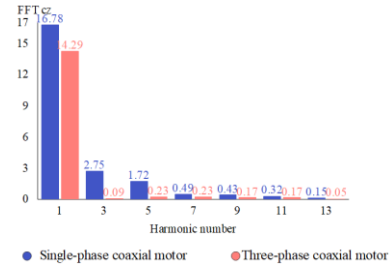

Fig. 7: Harmonic analysis of phase back

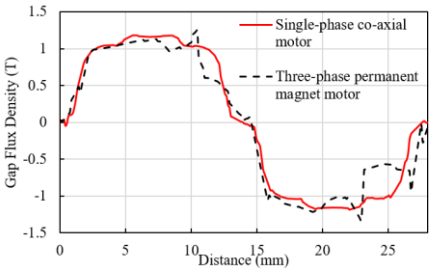

Fig. 8: Air-gap magnetic density

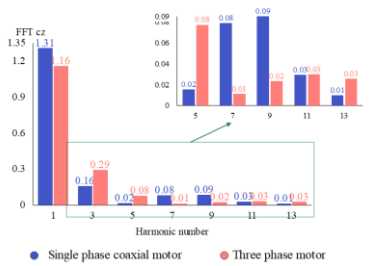

Fig. 9: Harmonic analysis of air-gap

Fig. 10 shows the magnetic field distribution of two kinds of motors under no-load state. The rotor core is partially saturated at the tangential magnetized permanent magnet and the stator is partially saturated at the tooth tip, but it has little impact on the electromagnetic torque production.

Fig. 11 (a) shows the waveforms of cogging torque of two kinds of motors. It can be seen that the peak-peak values of cogging torque of two kinds of motors are 2.6 N·m and 1.7 N·m respectively The cogging torque of three-phase coaxial permanent magnet motor is smaller.

b. The load performance contrast

In order to compare the torque output capacity of the two motors, two AFPM motors initially operate at the same current density and back EMF peak value at no load. In contrast, the single-phase coaxial motor has larger electromagnetic torque with less fluctuation, which means that when the two motors have the same volume, the single-phase coaxial motor has greater torque density and power density.

Fig. 11(b) shows that the output average torque of single-phase coaxial motor is about 28 N·m, and the output average torque of three-phase coaxial motor is relatively smaller, which is about 21 N·m. It can be seen that the output torque of single-phase coaxial motor is larger. Due to the influence of

electromagnetic coupling, part of the magnetic saturation state is offset, three-phase coaxial motor has smaller torque than single-phase coaxial motor.

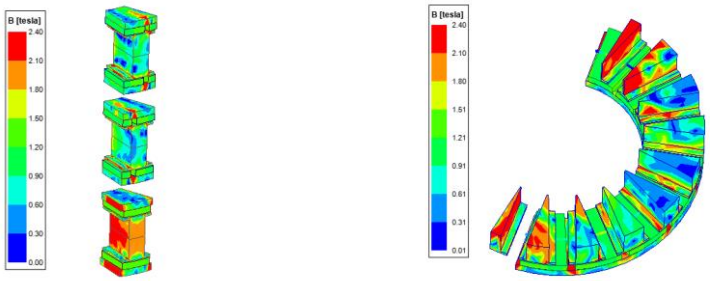

(a) Magnetic field of single-phase coaxial motor at no load

(b) Magnetic field of three-phase coaxial motor at no load

Fig. 10: Magnetic field distribution at no load

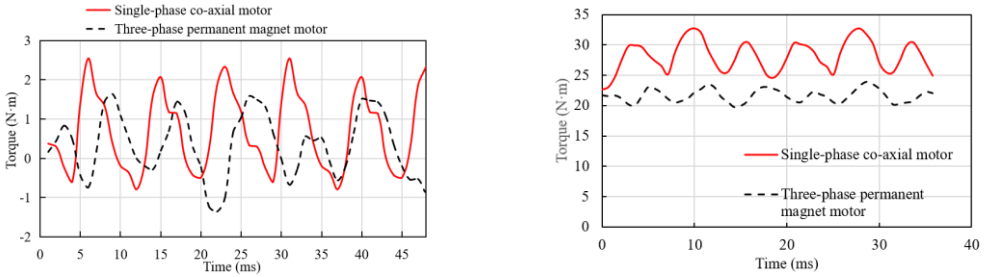

(a) No load cogging torque waveform.

(b) Electromagnetic torque waveforms.

Fig. 11 Motor torque curve

Fig. 12 shows that the stator teeth and stator yoke of the two motors which present have partial magnetic saturation. The result shows that the stator teeth and stator yoke of the two motors are partially magnetically saturated and the magnetic density saturation of the single-axis motors is relatively higher.

The average rated output power of three-phase coaxial motor and single-phase coaxial motor is 4.54 kW and 5.92 kW respectively. Through the average output power and effective material weight of the motor, we can obtain that the rated power density of the motor with two different topologies are 1.59 kW/kg and 2.00 kW/kg respectively. The result shows that single-phase coaxial motor has higher power density and higher material utilization than three-phase coaxial motor.

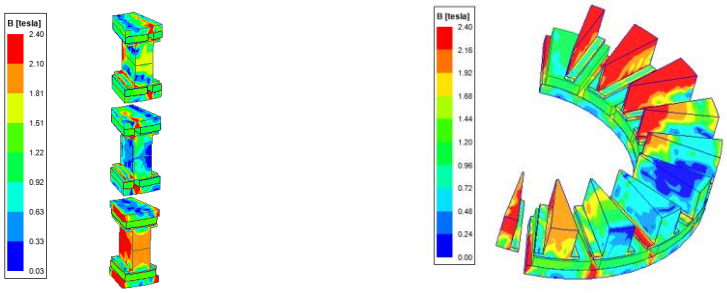

(a) Magnetic field of single-phase coaxial motor at load.

(b) Magnetic field of three-phase coaxial motor at load.

Fig. 12: Magnetic field distribution at load

In Fig. 13, the torque current ratio curve of single-phase coaxial motor and traditional three-phase coaxial motor (under id = 0 control) is compared. It can be seen from the figure that single-phase motor for coaxial cascade can produce higher torque under the same current.

Fig. 14 shows the power/torque speed curves of two different topologies of single-phase coaxial motor and three-phase coaxial motor. By observing the reverse electric momentum curve of the motor, changing the current and current angle of the motor, the torque curve at different speeds is obtained, and the power curve at different speeds is obtained through the calculation formula of torque and power. It shows that the topology of single-phase multistage series coaxial motor has better torque output capacity than the traditional three-phase series coaxial motor.

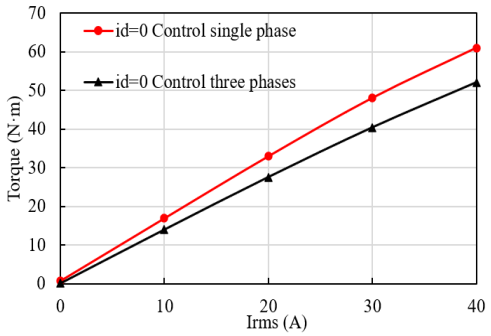

Fig. 13: Torque vs phase current curve (id = 0 control)

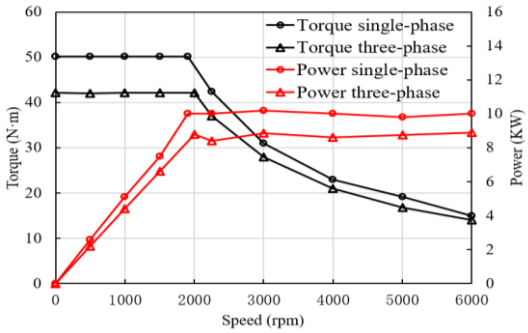

Fig. 14: Power / torque vs speed curves

c. Efficiency calculation of single-phase coaxial motor

The loss of the motor determines the efficiency of the motor, among which the core loss, permanent magnet eddy current loss and copper loss are the main parts of the total loss of the motor. Table IV shows the comparison of electro-magnetic performance parameters between single-phase coaxial motor and three-phase coaxial motor.

Table IV: The comparison of two motors

Parameter	Three-phase Coaxial Motor	Single-phase Coaxial Motor
No Load Back EMF	26.37 V	26.43 V
Rated Output Power	4.5 kW	5.9 kW
Power Density	1.59 kW/kg	2.00 kW/kg
Total Weight	2.848 kg	2.935 kg
Core Loss	2.7 W	2.5 W
Winding Loss	219 W	223 W
Eddy Current Loss	90 mW	120 mW
Total Loss	221.79 W	225.62 W
Motor Efficiency (η)	95.0 %	96.2 %

Conclusion

This paper compares traditional three-phase AFPM motor and single-phase AFPM motor for coaxial combination with the same material and size from the aspects of motor topology and electromagnetic performance. It is concluded that compared with three-phase AFPM motor, single-phase AFPM motor for coaxial combination has the higher output torque, the better no-load waveform. The power density of single-phase coaxial motor for coaxial cascading to form three-phase AFPM motor is increased by 25.8%. The efficiency of single-phase coaxial motor is 96.2%, which is higher than that of the traditional three-phase coaxial motor.

References

[1] B. B. Choi, “Propulsion Powertrain Simulator: Future turboelectric distributed-propulsion aircraft,” IEEE Electrification Magazine, vol.2, no.4, pp. 23-34, Dec. 2014: 10.1109/MELE.2014.2364901.

[2] K. P. Duffy and R. H. Jansen, “Turboelectric and Hybrid Electric Aircraft Drive Key Performance Parameters,”. 2018 AIAA/IEEE Electric Aircraft Technologies Symposium (EATS), 2018, pp. 1-19.

[3] S. Agrawal, A. Banerjee and R. F. Beach, “Brushless Doubly-Fed Reluctance Machine Drive for Turbo-Electric Distributed Propulsion Systems,”. 2018 AIAA/IEEE Electric Aircraft Technologies Symposium (EATS), 2018, pp. 1-17.

[4] C. Ye, Y. Du, J. Yang, X. Liang, F. Xiong and W. Xu,“Research of an Axial Flux Stator Partition Hybrid Excitation Brushless Synchronous Generator,” in IEEE Transactions on Magnetics Vol. 54, no. 11, pp. 1-4, Nov. 2018.

[5] W. Geng, J. Hou and Q. Li: “Electromagnetic Analysis and Efficiency Improvement of Axial-Flux Permanent Magnet Motor with Yokeless Stator by Using Grain-oriented Silicon Steel,” IEEE Transactions on Magnetics

[6] A.M.El-Refaie, “Fractional-slot concentrated-windings synchronous permanent magnet machines: Opportunities and challenges,” IEEE Trans .Ind. Electron., vol. 57, no. 1, pp. 107–121, Jan. 2010.

[7] H. S. Che, M. J. Duran, E. Levi, M. Jones, W. P. Hew and N. Abd Rahim, “Postfault Operation of an Asymmetrical Six-Phase Induction Machine with Single and Two Isolated Neutral Points,” IEEE Trans. on Power Electronics, vol.29, no.10, pp.5406-5416, Oct. 2014.

[8] M.Ruba and D. Fodorean, “Analysis of Fault-Tolerant Multiphase Power Converter for a Nine-Phase Permanent Magnet Synchronous Machine,” IEEE Trans. on Industry Appl., vol.48, no.6, pp.2092-2101,Nov.-Dec. 2012.

[9] M. Barcaro, N. Bianchi and F. Magnussen, “Six-Phase Supply Feasibility Using a PM Fractional-Slot Dual Winding Machine,” IEEE Trans. on Ind. Appl., vol.47, no.5, pp.2042-2050, Sept./Oct. 2011.

[10] Xuefeng Jiang; Wenxin Huang; Ruiwu Cao; Zhen yang Hao; Jie Li; Wen Jiang, “Analysis of a Dual-Winding Fault-Tolerant Permanent Magnet Machine Drive for Aerospace Applications,” IEEE Trans. On Magnetics, vol.51, no.11, pp.1-4, Nov. 2015.

[11] J. W. Bennett, G. J. Atkinson, B. C. Mecrow, D. J. Atkinson, “Fault-Tolerant Design Considerations and Control Strategies for Aerospace Drives,” IEEE Trans. on Industrial Electronics, vol.59, no.5, pp.2049-2058, May 2012.

[12] Vansompel, H.; Sergeant, P.; Dupre, L.; Bossche, A. “A Combined Wye-Delta Connection to Increase the Performance of Axial-Flux PM Machines with Concentrated Windings.” IEEE Trans. Energy Convers. 2012, 27, 403–410.